Clathrate Nature of the High-Pressure Tetrahydrofuran Hydrate Phase and Some New Data on the Phase Diagram of the Tetrahydrofuran−Water System at Pressures up to 3 GPa

Andrej Yu. Manakov,*,‡ Sergey V. Goryainov,# Alexandr V. Kurnosov,‡ Anna Yu. Likhacheva,# Yuri A. Dyadin,†,‡ and Eduard G. Larionov‡

Institute of Inorganic Chemistry, Siberian Branch of the Russian Academy of Sciences, Ac. Lavrentiev av. 3, 630090 Novosibirsk, Russia, and Institute of Mineralogy and Petrography, Siberian Branch of the Russian Academy of Sciences, Ac. Koptug av. 3, 630090, Novosibirsk, Russia

Received: April 23, 2002; In Final Form: November 6, 2002

Raman spectra of the internal vibrations of tetrahydrofuran molecules in two gas hydrate phases formed in the tetrahydrofuran−water system, as well as the spectra of solid and liquid tetrahydrofuran, under high-pressure conditions have been studied for the first time. A conclusion that the high-pressure hydrate is, most probably, of clathrate nature is made on the basis of spectral data. This hydrate is stable in the pressure range 0.49−3 GPa at room temperature. At a pressure of 3 GPa, the upper boundary (with respect to pressure) of the existence of the high-pressure hydrate is discovered. It corresponds to the decomposition of the hydrate into solid tetrahydrofuran and ice VII.

Introduction

Clathrate hydrates are the class of inclusion compounds in which the host framework is composed of water molecules and guest molecules occupy polyhedral cavities of this framework. In the case of gaseous (under normal conditions) guest molecules, these compounds are usually called gas hydrates. Because of the important role of gas hydrates in natural ecosystems and substantial resources of hydrocarbons in the form of gas hydrates in the Earth's crust, this class of compounds is the subject of increasing current interest.[1,2] The attention of researchers working in this area focuses mostly on the behavior of gas hydrates at moderate pressures because this pressure range is important for practical applications. However, investigations of these compounds at high pressures (above 0.1 GPa) are very informative and important for the understanding of general laws of supramolecular organization in the water−guest systems. The results of these studies also find application in other fields, for example, in planetology.[3] Detailed reviews of the modern state of clathrate hydrate chemistry are presented by several authors.[4−6]

Hydrates of cubic structure II (CS-II) with hydrate number (water/guest molar ratio) 17 are known to be formed at atmospheric pressure in guest−water binary systems if the van der Waals' diameter of the guest molecule is about 6−7 Å.[1] Known clathrate hydrate structures are considered in detail in ref 4. For three systems of this type (with propane, sulfur hexafluoride, and tetrahydrofuran, hereafter referred to as **THF**), the decomposition curves of gas hydrates formed at pressure up to 1.5 GPa have been investigated.[7,8] Three hydrate phases (**h_1**, **h_2**, **h_3**) can form in each system and are numbered according to the formation pressure in the ascending order; **h_1** hydrate is stable at ambient pressure. As the pressure increases, phases with denser lattice packing are formed. For the system with **THF**, approximate stoichiometry of all hydrate phases has been determined.[6] In the case of the **h_1** hydrate, the hydrate number is 17, which corresponds to the value expected for the CS-II hydrate. For the **h_2** hydrate, the hydrate number was found to be 7, which allowed the authors of ref 6 to describe this hydrate as a cubic structure I (CS-I) type. It was demonstrated by X-ray structural investigations that the **h_2** hydrate formed with tetrahydrofuran and sulfur hexafluoride does belong to CS-I.[9,10] Finally, for the **h_3** hydrate, the hydrate number was found to be 5, no information about the structure of this hydrate phase being available in the literature. A detailed consideration of the relationship between the density of clathrate hydrate structure packing and the behavior of hydrate-forming systems under pressure is presented in ref 6.

From the point of view of clathrate hydrate chemistry, an important difference between propane and sulfur hexafluoride is the presence of an oxygen atom in the heterocycle of **THF** molecule, this oxygen being able to form hydrogen bonds with water molecules. For this reason, hydrates of nonclathrate nature can also be formed in the **THF**−water system. As demonstrated in ref 11, the temperature dependence of the thermal conductivity of the **h_3** hydrate is similar to that of crystalline solids and differs from the dependence typical for clathrate hydrates, which exhibit an increase of thermal conductivity with temperature increase (glasslike behavior). However, the water content of the **h_3** hydrate is unusually high for nonclathrate hydrates of organic molecules in which water does not build a two- or three-dimensional framework. The water content of the **h_3** hydrate is close to the minimal amount necessary for the formation of hydrate framework with cavities of sufficient size to include **THF** molecules. An additional investigation of the **h_3** hydrate is of interest to make firm conclusion whether this compound has clathrate or nonclathrate nature.

Another problem that would be interesting to solve deals with the existence of an upper-pressure limit of gas hydrate stability. At present, it is known that gas hydrates with relatively small

* To whom correspondence should be addressed. Phone: (7-3832)39-13-46. Fax: (7-3832)34-44-89. E-mail: manakov@che.nsk.su.
† Deceased.
‡ Institute of Inorganic Chemistry.
# Institute of Mineralogy and Petrography.

10.1021/jp0259925 CCC: $25.00
Published on Web 07/12/2003

guest molecules (hydrogen, methane) exist up to pressures of several tens of gigapascals.[12,13] Probably, the same situation applies to systems with helium and argon, but hydrate formation in these systems at such pressures has not been studied.[14,15] In systems with hydrogen, helium, and methane, high-pressure phases are formed because of the intercalation of guest molecules into the cavities of the crystal framework of ices II, Ic, and Ih (most likely, a similar situation also takes place in the argon system[16]). In the case of larger molecules (such as **THF**, sulfur hexafluoride, etc.), one can hardly expect the formation of similar compounds. The achievable packing density in typical polyhedral gas hydrates is not high enough to allow these compounds to exist at pressures above several tens of gigapascals.[6,16] So, at some pressure, the decomposition of hydrate into components should occur, or a new, more tightly packed hydrate phase (probably semiclathrate or nonclathrate) should be formed. For the case of rather large guest molecules, this problem remains practically uninvestigated.

One of the most widespread techniques used to investigate high-pressure phenomena is Raman spectroscopy employing high-pressure diamond anvil cells. Recent papers in which this technique was used to study hydrate formation at high pressure in the argon−water system,[14] as well as a large number of works demonstrating the efficiency of Raman spectroscopy for the investigation of gas hydrates,[17,18,19] motivated us to apply to this technique to solve the problems met in our studies. The goal of the present investigation is to establish the nature of the $\mathbf{h_3}$ hydrate in the system **THF**−water (clathrate or nonclathrate) and to answer the question concerning the existence of the upper-pressure limit for hydrate formation in this system.

Experimental Section

Raman spectra were recorded with a DILOR OMARS 89 spectrometer equipped with a CCD Princeton Instruments LN/CCD1100PB detector. The 514.5 nm line of an argon ion laser was used for excitation. The detector was calibrated with the characteristic lines of a neon lamp. The uncertainty in the position of spectral bands was $\Delta\nu = \pm 0.5$ cm^{-1}. A detailed description of the high-pressure diamond anvil cell is given in ref 20. Pressure in the cell was measured from the baric shift of the R_1 and R_2 lines of ruby fluorescence using the pressure scale proposed in ref 21 ($\Delta\nu = \pm 0.5$ cm^{-1} corresponds to an error in the pressure determination of ± 0.07 GPa). For measurements at temperatures different from the room temperature (20 $\pm$ 1 °C), an air thermostat was used to maintain the required temperature with an accuracy of ± 0.5 °C. Tetrahydrofuran was purified from peroxides, dried with lithium alumohydride, and distilled twice. **THF** solutions in water were prepared by weight. The dissolved gases were removed from water and **THF** by boiling before they were mixed; the degassed solutions were stored in helium atmosphere. To investigate the spectra of the $\mathbf{h_3}$ hydrate, the cell was loaded with 75 mass % **THF** solution (in some experiments 40 mass % **THF** solution was used; we did not observe any substantial differences in the results of these experiments). Single crystals of the hydrate were grown from solution in several pressure increase−decrease cycles at a pressure of about 0.7 GPa and at room temperature (20 $\pm$ 1 °C). The spectra were recorded at constant temperature while increasing pressure by steps of 0.1−0.2 GPa. The band shift with pressure was investigated for the $\mathbf{h_3}$ phase, solid, and liquid **THF** at room temperature. In the last two cases, pure **THF** was loaded into the apparatus, but no single crystals were grown. When investigating the spectra of the $\mathbf{h_2}$ hydrate, a mixture with the composition corresponding to the ideal stoichiometry (**THF*7H$_2$O** corresponds to 36.3 mass % of **THF** in the solution) was loaded into the high-pressure apparatus; hydrate single crystal was grown under quasi-isochoric conditions at varied temperature. Melting temperature of this hydrate crystal coincided with the value expected for the $\mathbf{h_2}$ phase judging from the phase diagram. Two procedures were used to investigate the melting curve of pure **THF** under pressure. At pressures up to 0.8 GPa, measurements were carried out by means of differential thermal analysis (the procedure is described in ref 22). The accuracy of temperature determination was ± 0.25 °C, and that of pressure was ± 0.005 GPa. At higher pressures, measurements were carried out in diamond anvil cells. Pressure was decreased stepwise at constant temperature until the onset of crystal melting, which corresponds to a point on the monovariant curve in a single-component system. We estimate the accuracy of temperature and pressure measurement in these experiments as ± 0.5 °C and ± 0.07 GPa, respectively. Two points obtained by us on the decomposition curve of hydrate $\mathbf{h_3}$ were determined by raising temperature, volume of the high-pressure cell being practically constant. Points on the decomposition curve were determined by visual observation.

Results and Discussion

Spectra. We investigated the Raman spectra of the internal vibrations of **THF** molecules in two gas hydrates formed in the **THF**−water system ($\mathbf{h_2}$ and $\mathbf{h_3}$), as well as of solid and liquid **THF** (**s** and **lt**, respectively). Spectra obtained from the hydrate crystal could be clearly distinguished from those of the neighboring area enriched with **THF**. The dependence of the shifts of spectral bands on pressure was linear within experimental error for the spectra of all three investigated phases. The data are shown in Table 1 with typical spectra shown in Figure 1. The standard deviations of the parameters given in Table 1 include errors caused by uncertainty in the determination of the positions of the bands and errors in pressure determination. At a given pressure, the positions of the bands in the spectra of coexisting phases (for example, $\mathbf{h_3}$ and liquid water−**THF** mixture, hereafter referred to as **l**) were clearly distinguishable. A detailed consideration of the Raman spectra of the **THF** molecule in liquid, solid, and gaseous states was presented in ref 23; band assignment in the spectra investigated by us was based on the data of this study.

Tetrahydrofuran is a cyclic molecule with C_2 symmetry in both the liquid and solid state.[23,24] There are 33 internal vibrations $G(C_2) = 17A + 16B$. Let us consider the major bands of the Raman spectrum of solid **THF** at 4.08 GPa. Two narrow intense bands are observed at 891.5 and 950.3 cm^{-1} and a less intense band at 1066.4 cm^{-1}. These three modes correspond to symmetric stretching vibrations (A) of the heterocycle. A doublet at 1256.8 and 1270.7 cm^{-1} is related to twisting vibrations of CH_2 groups (with respect to the ring plane), assumed symmetry being A and B, respectively. Other vibrations of the CH_2 group, namely, rocking and wagging modes, are only weakly active in Raman spectra. The 1320−1350 cm^{-1} region in the Raman spectra was overlapped by the strong first-order band of diamond at 1330 cm^{-1} (Figure 1). The bending vibrations of CH_2 groups are observed in the region 1450−1550 cm^{-1}. The stretching C−H vibrations of the **THF** molecule are observed in the region 2850−3050 cm^{-1}. The spectra of pure crystalline **THF**, investigated by us at pressures up to 10.5 GPa and temperature 20 $\pm$ 1 °C, do not exhibit any qualitative differences from the spectra investigated at atmospheric pressure and low temperatures[23] (for details, see below). The dependence of the shift of spectral bands on pressure has no discontinuities, which would

TABLE 1: Raman Spectra of Liquid THF, Solid THF, and h_2 and h_3 Hydrates of THF[a]

solid **THF** (2.85−10.5 GPa)[b]		hydrate $\mathbf{h_3}$ (0.7−3 GPa)[b]		liquid **THF** (0.7−2.85 GPa)[b]		hydrate $\mathbf{h_2}$ (0.38 GPa, −65 °C)[c]
ν (cm^{-1}) at 1 bar	$\partial\nu/\partial P$ (cm^{-1} GPa^{-1})	ν (cm^{-1}) at 1 bar	$\partial\nu/\partial P$ (cm^{-1} GPa^{-1})	ν (cm^{-1}) at 1 bar	$\partial\nu/\partial P$ (cm^{-1} GPa^{-1})	ν (cm^{-1})
839(1) vw	2.1(2)					
863(3) vw	0.3(7)	917.9(7) vs	2.5(4)	898(2) sh	2(1)	898.3 sh
884.8(4) vs	2.0(1)	919(6) sh	5(2)	914(2) vs	6(1)	915.3 vs
924(2) vw	1.5(4)			945(1) vw	7.9(7)	
933.4(8) vs	4.2(1)					
960(1) vw	2.7(3)					
1046.9(8) mw	4.8(1)	1033.7(6) mw	5.8(3)	1028(1) mw	7.1(6)	1029.1 mw
		1072(2) vw	3(1)	1064(1) vw	3.1(5)	1062.5 vw
1145.4(2) w	0.9(1)			1139(2) vw	2(1)	
1181.2(7) vw	2.1(1)			1179(2) vw	2(1)	1170 vw
1199.2(8) w	3.9(1)					
1244.7(8) mw	3.0(1)	1222(2) sh	1(1)	1224(3) sh	5(1)	1223.6 mw
1259.6(3) mw	2.3(1)	1251(1) sh	1.0(7)	1244(2) mw	3(1)	1239.8 sh
1376(1) vw	2.2(2)					
1474.5(5) mw	1.9(1)	1446.9(4) mw	1.1(3)	1445(1) mw	1.9(4)	1446.5 mw
1483.3(7) vw	3.1(1)	1472(3) vw	0(2)	1482(2) sh	7(1)	1459.9 sh
1500.3(8) vw	3.3(1)	1488(2) vw	0(1)			1477.3 sh
						1488.3 w
2737.1(9) w	3.9(2)	2723(2) vw	1(1)	2719(1) vw	6.3(5)	2709 w
2870.3(9) vs	5.7(2)	2878(2) vs	4(1)	2867(1) vs	11.5(3)	2877.3 vs
2935(1) vs	5.2(2)	2916(2) mw	2(1)	2944(3) vs	2(2)	2914.5 sh
2953(3) sh	8.2(5)	2944(1) sh	3.6(4)	2976(1) vs	14.7(7)	2941.6 vs
2962(2) vs	10.1(3)	2964(1) vs	5.2(3)			2964.7 vs
3008(2) vs	7.7(3)	2961(2) vs	12(1)			2992.6 vs
		2987(2) vs	14(1)			

[a] Standard deviations of corresponding values are given in parenthesis. [b] Pressure intervals in which the spectra were studied. [c] Conditions at which the spectrum was recorded.

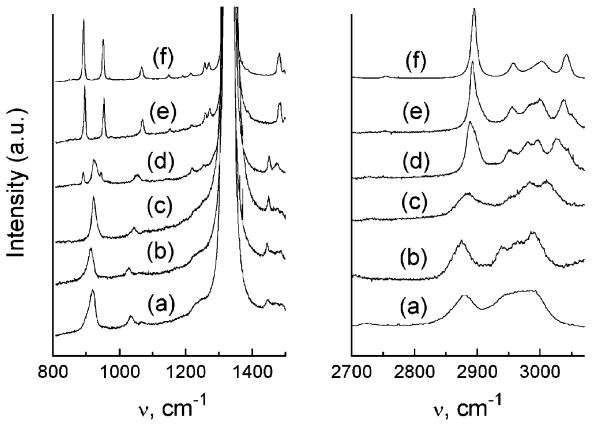

Figure 1. Typical Raman spectra of **THF** in the regions 800−1500 cm^{-1} (left) and 2700−3100 cm^{-1} (right). A very strong band at 1330 cm^{-1} corresponds to C−C stretch vibrations in diamond: (a) pure liquid **THF** at 0.92 GPa and room temperature; (b) the hydrate $\mathbf{h_2}$ at 0.38 GPa and −65 °C; (c) the hydrate $\mathbf{h_3}$ at 1.3 GPa and room temperature; (d) the hydrate $\mathbf{h_3}$ in the course of decomposition at 3.03 GPa and room temperature; (e) the decomposed hydrate $\mathbf{h_3}$ at 3.93 GPa (solid **THF**−ice mixture); (f) solid **THF** at 4.08 GPa.

be an evidence of possible phase transformations. Attention should be paid to the similarity between the spectra of **lt**, $\mathbf{h_2}$, and $\mathbf{h_3}$ phases and between these spectra and the spectra of the liquid **THF** at atmospheric pressure[23] and high pressures; at the same time, the spectra of the **s** phase exhibit substantial differences (Figure 1). Relative shift of bands in the spectra of **lt**, $\mathbf{h_2}$, and $\mathbf{h_3}$ phases is not large, and the bands are noticeably broadened. Substantial overlapping of bands is characteristic of the spectra. Only the band at about 1030 cm^{-1} remains practically free from overlap with the neighboring bands. The half-width of this band in the spectra of the **lt**, $\mathbf{h_2}$ and $\mathbf{h_3}$ phases is about 16 cm^{-1}, while the **s** phase exhibits the width close to 7 cm^{-1} (the instrumental bandwidth is about 3 cm^{-1}). No substantial changes of bandwidth occur with changing pressure. Taking into account the fact that the broadening of bands in the spectra of liquids and molecular crystals is usually caused by the dynamic disordering of molecules, one can conclude that the **THF** molecules in the $\mathbf{h_3}$ hydrate are disordered. The positions of bands contributing substantially to the breathing vibrations of the **THF** heterocycle (correspondingly, leading to the largest change in the molecule volume), as well as the bands corresponding to the stretching vibrations of C−H bonds, are most sensitive to pressure changes (Table 1). The absolute values of band shifts with pressure are smaller for hydrate phase than for the liquid one. As demonstrated in ref 23, a very interesting feature of the spectra of liquid **THF** at room temperature is the appearance of several bands as one intensive band at approximately 920 cm^{-1} (both at high and low pressure). All of these bands are resolved in the spectra of the solid **THF**. On temperature decrease, the bands in the spectra of the liquid phase begin to separate from each other (a shoulder appears at the high-frequency side). We also found a similar change in the spectrum of liquid **THF** on pressure increase (Figure 1). The authors of ref 25 observed the appearance of a similar shoulder in the spectra of the **THF** incorporated in the CS-II clathrate hydrate ($\mathbf{h_1}$ phase) on temperature decrease, the outline of the spectrum in this case being undoubtedly similar to the spectrum of the liquid **THF**. The observed splitting of the band at about 920 cm^{-1} in the spectrum of liquid **THF** and the above-mentioned features of band shift with pressure increase are, probably, caused by stronger interaction of **THF** molecule with neighboring molecules provided by compression or temperature

decrease. Band shifts caused by these reasons differ from each other, thus resulting in the observed splitting. The behavior of this band is strikingly different in the spectra of the $\mathbf{h_3}$ phase, in which no substantial asymmetry is exhibited within the entire pressure range in which the hydrate exists. In ref 26 the appearance of the shoulder at this band is explained by the formation of water−**THF** hydrogen bond. This explanation cannot be applied to our case because we observed the appearance of the shoulder in the spectrum of pure **THF**.

To summarize, the spectra of **THF** molecules in the $\mathbf{h_3}$ phase exhibit the following features: the appearance of the spectra is characteristic of compounds with disordered **THF** molecules; besides, the absence of splitting of the band at 920 cm^{-1} probably indicates that the **THF** molecule is located in a relatively rigid cage. To our opinion, the most probable explanation of these features is the clathrate (or, probably, semiclathrate) nature of the $\mathbf{h_3}$ hydrate, which is in good agreement with the similarity between the spectrum of this phase and the spectra of clathrate hydrates $\mathbf{h_1}$ and $\mathbf{h_2}$. We believe that this conclusion does not contradict the results presented in ref 11 because the properties of the closely packed high-pressure hydrate phases can be expected to be intermediate between the properties of typical gas hydrates and the properties of the typical solid phases, as it was found in ref 11. Spectral bands of gas hydrates in which guest molecules occupy different types of cavities are usually split, corresponding to different surroundings of the guest molecules. Because no such splitting was observed in the spectra of $\mathbf{h_2}$ and $\mathbf{h_3}$ phases investigated by us, we can assume that only one type of cavity is filled with **THF** molecules in both phases. For the $\mathbf{h_2}$ hydrate related to the cubic structure I, this assumption is quite reasonable because the size of the small pentagondodecahedral cavity is obviously too small to enclose the **THF** molecule. We noted that if an air bubble is allowed into the high-pressure cell, the temperature of $\mathbf{h_2}$ hydrate decomposition increases (the hydrate stabilizes by filling empty cavities with nitrogen and oxygen molecules), while the temperature of $\mathbf{h_3}$ hydrate decomposition remains unchanged. On the basis of this observation, we can assume that most probably no vacant cavities are present in the structure of $\mathbf{h_3}$ hydrate.

Phase Diagram. The phase diagram of the tetrahydrofuran−water system, supplemented by our data for the pressures above 1 GPa, is shown in Figure 2. The following supplements have been made: (1) the upper-pressure limit for the existence of the $\mathbf{h_3}$ hydrate is discovered (a monovariant line $\mathbf{i_{VII}h_3s}$); (2) a region of syntectic decomposition of the $\mathbf{h_3}$ hydrate into water-enriched and **THF**-enriched liquid phases is found; (3) The melting curve of pure **THF** is investigated at pressures up to 2.5 GPa. A more detailed discussion of the results is given below.

Because we failed to find any literature data on the phase diagram of pure **THF** at high pressure, we obtained this information as a part of our work. Numerical data for the melting curve of pure **THF** below a pressure of 2.5 GPa are shown in Table 2. The melting curve of pure **THF** does not have any characteristic features that could be evidence of polymorphous phase transitions (similar conclusion can be made from the spectral data). So we conclude on the basis of our results that within the investigated pressure (up to 10.5 GPa) and temperature (−108 to 80 °C) ranges it is very probable that only one phase of the solid **THF** is stable, in which the packing motif is close to that investigated at atmospheric pressure and low temperature.[24] It should be noted that pure **THF**, as well as

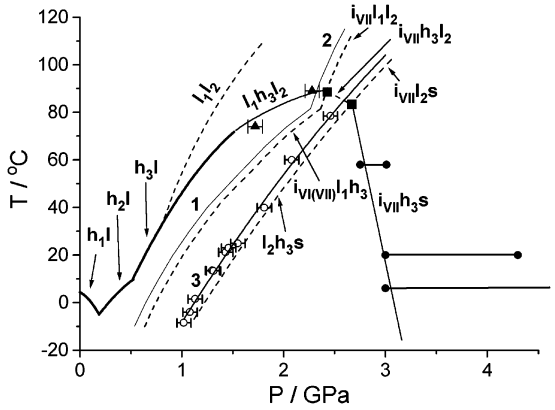

Figure 2. Phase diagram of **THF**−water system at high pressures: $\mathbf{h_1}$, $\mathbf{h_2}$, $\mathbf{h_3}$ = **THF** hydrates; $\mathbf{i_n}$ = ices; $\mathbf{l_1}$, $\mathbf{l_2}$ = liquids (water-rich and **THF**-rich, respectively); **s** = solid **THF**. Curves 1 and 2 correspond to melting of ices VI and VII, respectively; curve 3 corresponds to melting of **THF**. Experimental points are identified as follows: (○) melting of **THF**; (●) decomposition of $\mathbf{h_3}$ hydrate ($\mathbf{i_{VII}h_3s}$), lines between the points showing the pressure intervals in which decomposition of the h_3 hydrate proceeds; (▲) decomposition of $\mathbf{h_3}$ hydrate ($\mathbf{l_1h_3l_2}$). The dashed lines are drawn schematically.

TABLE 2: The Melting Curve of THF in the Pressure Range from 0.03 to 2.46 GPa

DTA[a]		DAC[a]	
P (GPa)	*T* (°C)	*P* (GPa)	*T* (°C)
0.03	−102.4	0.990	−13.1
0.05	−100.3	1.020	−8.5
0.096	−94.1	1.080	−4.0
0.192	−85.1	1.130	1.5
0.347	−68.6	1.300	13.5
0.462	−57.5	1.310	13.3
0.587	−46.0	1.430	21.2
0.720	−35.0	1.460	23.0
0.806	−26.7	1.550	24.9
		1.810	39.9
		2.080	60.0
		2.460	78.5

[a] DTA = differential thermal analysis; DAC = visual observations in diamond anvil cell.

THF-enriched liquid phase, tends to form a superpressurized liquid up to 2 GPa.

While attempting to grow $\mathbf{h_3}$ hydrate crystals at temperatures above 30 °C and at pressures corresponding to the decomposition curve of this hydrate, we observed the formation of platelet-shaped crystals. The melting curve of these crystals coincided within experimental error with the melting curve of ice at corresponding temperatures and pressures. It was also found that melting of the $\mathbf{h_3}$ hydrate at temperatures above 30 °C was sometimes accompanied by the formation of rapidly disappearing liquid−liquid boundaries (as observed visually). To our opinion, these observations can be explained only by the coexistence of immiscible water-rich and **THF**-rich liquids at these conditions, which corresponds to the transition from congruent melting of the $\mathbf{h_3}$ hydrate to syntectic decomposition. We did not succeed in investigation of the layering region in detail; the $\mathbf{l_1l_2}$ critical locus of liquid−liquid equilibrium is shown only schematically in the phase diagram.

At room temperature, the $\mathbf{h_3}$ hydrate crystal coexists with **THF**-rich liquid and solid phases within a pressure range from 0.7 to about 3 GPa. No qualitative changes were observed in the system in this region. The shape of the crystal, observed visually, can be characterized as a distorted hexagonal prism. A linear dependence of shifts of the spectral bands on pressure

indicates that the system does not contain any unknown hydrate phases. Transformations accompanied by substantial changes in the spectrum at a pressure of 3.0 GPa signal the upper-pressure limit of hydrate stability above which the phases coexisting in the system are ice VII and solid **THF** (Figure 1). Microscope observations allowed us to observe cracking of the crystal. The most apparent changes in the spectrum were the splitting of the intense band at ~920 cm^{-1} on pressure increase, which was used as indication of hydrate decomposition at temperatures different from the room temperature. At room temperature, the positions of new peaks corresponded within experimental error to those in the spectra of pure solid **THF** at a given pressure. With further increase in pressure, the peaks corresponding to the hydrate phase disappeared completely; the spectrum then completely corresponded to the spectrum of solid tetrahydrofuran at the given pressure. It is interesting to note that when the pressure was increased to 3.5 GPa, the region of coexistence of the hydrate and liquid phase (with excess **THF**) remained metastable and the hydrate did not decompose until **THF** crystallized. As soon as the liquid-phase crystallized, the crystal decomposed very rapidly.

The investigation of the hydrate decomposition was performed at four temperatures: 58, 20, 6, and −5 °C. The point at which the peaks corresponding to solid **THF** appeared was taken as the start of decomposition; the point at which the peaks corresponding to the hydrate phase disappeared completely meant the end of decomposition (at temperatures 58 and 20.5 °C). The extension of this phase transition with respect to pressure is a purely kinetic effect because the coexistence of hydrate and products of its decomposition (solid **THF** and ice) is thermodynamically possible only at the curve in the $P-T$ section (this means a point at isothermal compression). At a temperature of 58 °C, decomposition was observed within a pressure range of 2.75−3.01 GPa and at 20 °C within the range 3.0−4.3 GPa. At 6 °C, the start of decomposition was observed at a pressure of 3.0 GPa, but the peaks corresponding to the hydrate phase did not disappear at a subsequent pressure increase to 5 GPa. At −5 °C, no hydrate decomposition was observed up to the upper limit of the investigated region (4.6 GPa). A probable explanation of the observed phenomena is slow kinetics of transformation when both the initial reagents and the final products are solid, especially at temperatures much lower than the temperature of $\mathbf{h_3}$ hydrate decomposition. It is likely that the nature of this behavior of tetrahydrofuran hydrate is similar to the phenomena discovered in isothermal compression of ice Ih.[27,28] At sufficiently high temperatures, transformations that occur at isothermal compression of the compound correspond to thermodynamic equilibrium (in the case under consideration, decomposition of hydrate into solid **THF** and ice). With decreasing temperature, the decreasing amplitude of thermal vibrations of water molecules makes thermodynamically controlled phase transitions impossible. The phase remains in a metastable state until the loss of mechanical stability (amorphization). We did not reach this limit in our experiments.

On the basis of these data, taking into account the fact that the three-phase curves $\mathbf{i_{VI}l_1h_3}$ **(**$\mathbf{i_{VII}l_1h_3}$**)** and $\mathbf{h_3l_2s}$ in the $P-T$ projection of the phase diagram are close to the corresponding single-component melting curves $\mathbf{i_{VI}l}$ **(**$\mathbf{i_{VII}l}$**)** and **ls**, the outline of the phase diagram in high-pressure region (1.5−4.0 GPa) suggested above, the existence of quadrupole points $\mathbf{i_{VII}h_3l_1l_2}$ and $\mathbf{i_{VII}h_3ls}$, and their approximate position (Figure 2) seem reasonable. The supposed three-phase curves are designated with dashed lines, directions being shown in agreement with Schreinemakers' rules. To test the behavior of the hydrate decomposition curve at pressures above the region investigated earlier,[29] two points of this equilibrium were obtained, their position being in good agreement with the expected behavior.

Conclusions

In the present investigation, we succeeded in determining the type of the phase diagram of the tetrahydrofuran−water system in the high-pressure region. For the first time, the upper-pressure limit of the $\mathbf{h_3}$ hydrate existence region is discovered; it corresponds to the monovariant curve $\mathbf{i_{VII}h_3s}$. It is suggested that the hydrate $\mathbf{h_3}$ has a clathrate nature relying on the similarity between the spectra of **THF** molecule trapped in this hydrate and the spectra of this molecule in the clathrate hydrate $\mathbf{h_2}$ and the liquid phase.

Acknowledgment. This work was supported by Grant of Presidium SD RAS No. 147 and RFBR Grants 02-05-65313 and 00-03-32563. S.V.G and A.V.K. thank Grant CRDF Nr REC-008 for financial support. Authors thank Dr. J. L. Hutter for help in preparation of the manuscript.

References and Notes

(1) Ripmeester, J. A. In *Gas Hydrates. Challenges for the Future*; Holder, G. D., Bishnoi, P. R., Eds.; Annals of the New York Academy of Sciences, Vol. 912; New York Academy of Sciences: New York, 2000; p 1.

(2) Kvenvolden, K. A. In *Gas Hydrates. Challenges for the Future*; Holder, G. D., Bishnoi, P. R., Eds.; Annals of the New York Academy of Sciences, Vol. 912; New York Academy of Sciences: New York, 2000; p 17.

(3) Anderson, J. D.; Lau, E. L.; Sjogren, W. L.; Schubert, G.; Moore, W. B. *Science* **1997**, *276*, 1236.

(4) Jeffrey, G. A. In *Comprehensive Supramolecular Chemistry*; Atwood, J. L., Davis, J. E. D., MacNicol, D. D., Vogtle, F., Eds.; Elsevier: New York, 1996; Vol. 6, p 115.

(5) Sloan, E. D., Jr. *Clathrate Hydrates of Natural Gases*, 2nd ed.; Marcel Dekker: New York, 1997.

(6) Dyadin, Yu. A.; Bondaryuk, I. V.; Zhurko, F. V. In *Inclusion Compounds*; Atwood, J. L., Davis, J. E. D., MacNicol, D. D., Eds.; Oxford University Press: Oxford, U.K., 1991; Vol. 5, p 213.

(7) Larionov, E. G.; Manakov, A. Yu.; Dyadin, Yu. A.; Zhurko, F. V. In *Gas Hydrates. Challenges for the Future*; Holder, G. D., Bishnoi, P. R., Eds.; Annals of the New York Academy of Sciences, Vol. 912; New York Academy of Sciences: New York, 2000; p 967.

(8) Dyadin, Yu. A.; Larionov, E. G.; Aladko, E. Ya.; Zhurko, F. V. *Dokl.Phys. Chem.* **2001,** *376* (1−4), 23.

(9) Zakrewski, M.; Klug, D. D.; Ripmeester, J. A. *J. Inclusion Phenom. Mol. Recognit. Chem.* **1994**, *17*, 237.

(10) Manakov, A. Yu.; Larionov, E. G.; Ancharov, A. I.; Mirinskii, D. S.; Kurnosov, A. V.; Dyadin, Yu. A.; Tolochko, B. P.; Sheromov, M. A. *Mendeleev Commun.* **2000**, 235.

(11) Ross, R. G.; Andersson, P. *Can. J. Chem.* **1982**, *60*, 881.

(12) Vos, W. L.; Finger, L. W.; Hemley, R. J.; Mao, H. *Phys. Rev. Lett.* **1993**, *71* (19), 3150.

(13) Loveday, J. S.; Nelmes, R. J.; Guthrie, M.; Klug, D. D.; Tse, J. S. *Phys. Rev. Lett.* **2001**, *87* (21), 215501.

(14) Lotz, H. T.; Schouten, J. A. *J. Chem. Phys*. **1999**, *111* (22), 10242.

(15) Londono, D.; Kuhs, W. F.; Finnej, J. L. *Nature* **1988**, *332*, 141.

(16) Dyadin, Yu. A.; Larionov, E. G.; Manakov, A. Yu.; Zhurko, F. V.; Aladko, E. Ya.; Mikina, T. V.; Komarov, V. Yu. *Mendeleev Commun*. **1999**, 209.

(17) Nakano, S.; Moritoki, M.; Ohgaki, K. *J. Chem. Eng. Data* **1999**, *44*, 254.

(18) Subramanian, S.; Kini, R. A.; Dec, S. F.; Sloan, E. D. *Chem. Eng. Sci.* **2000**, *55*, 1981.

(19) Tulk, C. A.; Ripmeester, J. A.; Klug, D. D. In *Gas Hydrates. Challenges for the Future*; Holder, G. D., Bishnoi, P. R., Eds.; Annals of the New York Academy of Sciences, Vol. 912; New York Academy of Sciences: New York, 2000; p 859.

(20) Goryainov, S. V.; Belitsky, I. A. *Phys. Chem. Miner*. **1995**, *22*, 443.

(21) Munro, R. G.; Piermarini, G. J.; Block, S.; Holzapfel, W. B. *J. Appl. Phys.* **1985**, *57* (2), 165.

(22) Dyadin, Yu. A.; Larionov, E. G.; Mirinskii, D. S.; Mikina, T. V.; Aladko, E. Ya.; Starostina, L. I. *J. Inclusion Phenom. Mol. Recognit. Chem.* **1997**, *28*, 271.

(23) Cadioli, B.; Gallinella, E.; Coulombeau, C.; Jobic, H.; Berthier, G. *J. Phys. Chem.* **1993**, *97*, 7844.

(24) Luger, P.; Buschmann, J. *Angew. Chem., Int. Ed. Engl.* **1983**, *22* (5), 410.

(25) Tulk, C. A.; Klug, D. D.; Ripmeester, J. A. *J. Phys. Chem. A* **1998**, *102* (45), 8734.

(26) Subramanian, S.; Sloan, E. D. *J. Phys. Chem. B* **2002**, *106*, 4348.

(27) Mishima, O. *Nature* **1996**, *384*, 546.

(28) Tse, J. S.; Klug, D. D.; Tulk, C. A.; Swainson, I.; Svensson, E. C.; Loong, C. K.; Shpakov, V.; Belosludov, V. R.; Belosludov, R. V.; Kawazoe, Y. *Nature* **1999**, *400*, 647.

(29) Dyadin, Yu. A.; Larionov, E. G.; Manakov, A. Yu.; Zhurko, F. V. *Mendeleev Commun.* **1999**, 80.